

## Transient band bending in a staggered-alignment type-II multiple-quantum-well structure

Fumio Sasaki, Tomobumi Mishina, and Yasuaki Masumoto  
*Institute of Physics, University of Tsukuba, Tsukuba, Ibaraki 305, Japan*  
 (Received 9 August 1990)

We observed a critical change of luminescence spectra under high-density excitation in staggered-alignment type-II  $\text{Al}_{0.34}\text{Ga}_{0.66}\text{As-AlAs}$  multiple quantum wells. Under the same density excitation ( $\sim 10 \mu\text{J cm}^{-2}$ ), a redshift of the  $\Gamma$ - $\Gamma$  luminescence and saturation of the  $X$ - $\Gamma$  luminescence were observed. Simultaneously, a blueshift of the  $X$ - $\Gamma$  luminescence was observed in the time-resolved spectrum. These phenomena show the carrier-induced transient band bending caused by real-space charge transfer through the interface.

Recently, an ultrafast pump-and-probe technique was adopted to study the dynamical aspects of staggered-alignment type-II superlattices and multiple quantum wells (MQW).<sup>1-3</sup> In this system, the  $\Gamma$ -electron state in the well layers has higher energy than the  $X$ -electron state in the barrier layers, so that the  $\Gamma$  electrons in the wells are scattered to the  $X$ -electron state through the interface. Real-space charge transfer takes place in the ultrafast, subpicosecond or picosecond, time domain depending on the penetration depth of the  $\Gamma$  electron to the barrier layers.<sup>3</sup> The scattered  $X$  electrons in the AlAs layers are combined with the  $\Gamma$  heavy hole in the well layers. The lifetime of the indirect luminescence ranges from submicrosecond to millisecond depending on the degree of the  $\Gamma$ - $X$  mixing, bath temperature, and sample quality.<sup>4-7</sup> On the other hand, the  $\Gamma$ - $\Gamma$  luminescence lifetime is as short as the  $\Gamma$ - $X$  scattering time.<sup>2,3,8</sup> Therefore, holes distribute in the well layers and some electrons in the barrier layers.

The spatial separation of carriers can induce a local electric field across the interface. As a result, carrier-induced band bending is expected in staggered-alignment type-II MQW or superlattices. Such transient band bending has a potential for device application. However, such a transient band bending has not been observed yet.

In the previous paper, we observed anomalous induced absorption at the low-energy tail of the  $\Gamma$ - $\Gamma$  exciton and suggested transient band bending as its origin.<sup>9</sup> In this paper, we confirm the transient band bending by means of luminescence spectroscopy in the staggered-alignment type-II  $\text{Al}_{0.34}\text{Ga}_{0.66}\text{As-AlAs}$  ternary-alloy multiple-quantum-well structure. The sample has 100 alternate layers of 9.2 nm ( $=L_w$ ) undoped  $\text{Al}_{0.34}\text{Ga}_{0.66}\text{As}$  and 2.7 nm ( $=L_b$ ) undoped AlAs. The background impurity concentration is less than  $5 \times 10^{15} \text{ cm}^{-3}$ . The sample directly immersed in liquid helium was excited by the frequency-doubled output of a  $Q$ -switched  $\text{Nd}^{3+}:\text{YAG}$  laser (where YAG is yttrium aluminum garnet) with a 3 ns pulse width. The pump power density ranges from  $1 \mu\text{J cm}^{-2}$  to  $140 \text{ mJ cm}^{-2}$ .

The photoluminescence spectra are shown in Fig. 1. The high-energy luminescence peak represents the  $\Gamma$ - $\Gamma$  transition and the low-energy peak the  $X$ - $\Gamma$  transition.<sup>10</sup> The relative intensity of the two peaks depends on the temperature and the excitation conditions such as the ex-

citation density and the pulse repetition. The figure shows the saturation of the  $X$ - $\Gamma$  luminescence. This is due to the long lifetime of the  $X$ -point luminescence on the order of  $10 \mu\text{s}$ . In contrast the  $\Gamma$ - $\Gamma$  luminescence intensity grows supralinearly.

The critical change of the luminescence spectrum takes place under excitation densities between 7 and  $30 \mu\text{J cm}^{-2}$ . The values correspond to carrier densities between  $3 \times 10^{11}$  and  $12 \times 10^{11} \text{ cm}^{-2}$ . With the increase of the excitation density, the  $\Gamma$ - $\Gamma$  luminescence peak shifts toward the lower energy. On the other hand, the  $X$ - $\Gamma$  luminescence does not shift and is saturated.

Figure 2 shows the  $\Gamma$ - $\Gamma$  peak energy (open triangles) and the spectrally integrated  $X$ - $\Gamma$  luminescence intensity

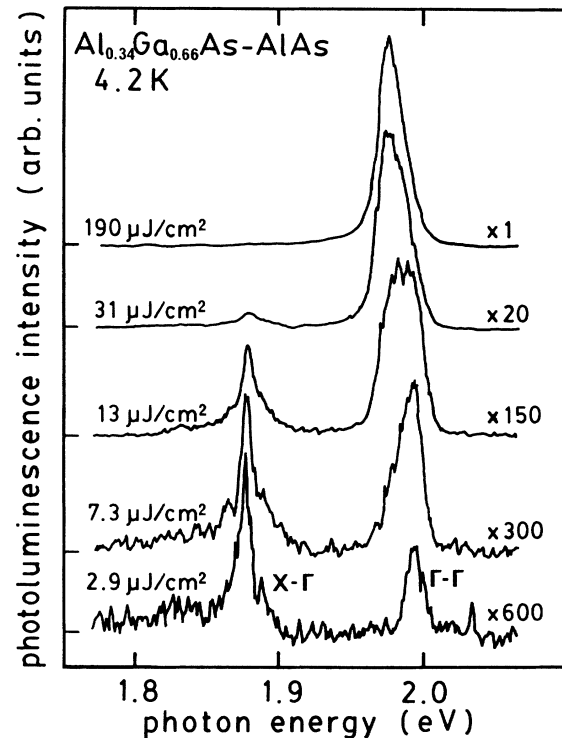


FIG. 1. Photoluminescence spectra of  $\text{Al}_{0.34}\text{Ga}_{0.66}\text{As-AlAs}$  MQW. The high-energy peak represents the  $\Gamma$ - $\Gamma$  transition and the low-energy peak the  $X$ - $\Gamma$  transition.

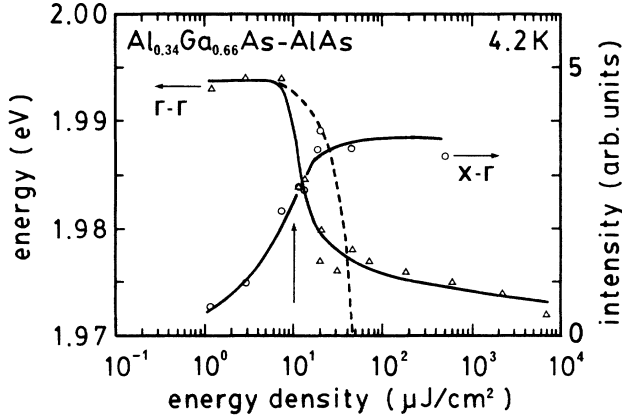


FIG. 2. Excitation-density dependence of the  $\Gamma$ - $\Gamma$  luminescence peak shift and the  $X$ - $\Gamma$  luminescence intensity. Open triangles represent the  $\Gamma$ - $\Gamma$  luminescence peak energy and open circles the  $X$ - $\Gamma$  luminescence intensity. The dashed line represents the result of the calculation with no adjustable parameters (see text). The vertical arrow represents the critical saturation density of the  $X$ - $\Gamma$  luminescence.

(open circles) as a function of the excitation density. The  $\Gamma$ - $\Gamma$  peak shift and the saturation of the  $X$ - $\Gamma$  luminescence take place under the same critical excitation density,  $10 \mu\text{J cm}^{-2}$ . This fact indicates that the origin of both phenomena is the same.

The photoexcited  $\Gamma$  electrons in the  $\text{Al}_{0.34}\text{Ga}_{0.66}\text{As}$  layers are scattered to the  $X$ -point of the AlAs layers with a time constant of 1.2 ps.<sup>3</sup> After a considerable amount of real-space charge transfer takes place, the electron distribution in the AlAs layers and the hole distribution in  $\text{Al}_{0.34}\text{Ga}_{0.66}\text{As}$  are considered to induce a local electric field. The potential energy and the electric field are obtained by solving the Poisson equation,

$$d^2V(z)/dz^2 = 4\pi\rho(z)/\epsilon_s. \quad (1)$$

Here,  $z$ ,  $V(z)$ ,  $\rho(z)$ , and  $\epsilon_s$  denote the quantum-well growth direction, the potential energy, the charge density, and the static dielectric constant, respectively. For simplicity, we assumed a uniform distribution of electrons in the AlAs layers and holes in the  $\text{Al}_{0.34}\text{Ga}_{0.66}\text{As}$  layers. In this case, the potential energies of the  $\Gamma$  electrons ( $V_{\Gamma e}$ ) and  $\Gamma$  holes ( $V_{\Gamma h}$ ) in the  $\text{Al}_{0.34}\text{Ga}_{0.66}\text{As}$  layers and the  $X$  electrons ( $V_{Xe}$ ) in the AlAs layers are modified from these unperturbed values  $V_{\Gamma e}^0$ ,  $V_{\Gamma h}^0$ , and  $V_{Xe}^0$  as follows:

$$\begin{aligned} V_{\Gamma e} &= V_{\Gamma e}^0 + (4\pi e^2 n_h / \epsilon_{sw}) z^2, \\ V_{\Gamma h} &= V_{\Gamma h}^0 + (4\pi e^2 n_h / \epsilon_{sw}) z^2, \\ V_{Xe} &= V_{Xe}^0 - (4\pi e^2 n_e / \epsilon_{sb}) z^2. \end{aligned} \quad (2)$$

The origin of the  $z$  axis is at the center of the  $\text{Al}_{0.34}\text{Ga}_{0.66}\text{As}$  layers for  $V_{\Gamma e}$  and  $V_{\Gamma h}$ , and at the center of the AlAs layers for  $V_{Xe}$ . Here,  $n_e$ ,  $n_h$ ,  $\epsilon_{sw}$ , and  $\epsilon_{sb}$  denote the three-dimensional electron density in the AlAs layers, the three-dimensional hole density in the  $\text{Al}_{0.34}\text{Ga}_{0.66}\text{As}$  layers, the dielectric constant in the  $\text{Al}_{0.34}\text{Ga}_{0.66}\text{As}$  layers and that in the AlAs layers, respectively. The potential profile of this model is schematically shown in Fig. 3.

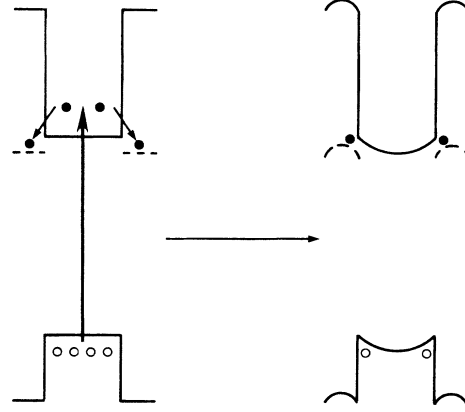


FIG. 3. Schematic change of the potential profile based on a transient band bending model.

We estimate the energy shift of the  $\Gamma$ - $\Gamma$  transition by using a perturbation calculation in an infinite-quantum-well structure. In our sample the penetration probability of  $\Gamma$  electrons in the AlAs layers and  $X_z$  electrons in the  $\text{Al}_{0.34}\text{Ga}_{0.66}\text{As}$  layers are estimated to be 0.75% and 3.0%, respectively.<sup>3</sup> The infinite-quantum-well model is considered to be sufficient for the order estimation because of the small penetration probabilities. Perturbations are represented by  $V_{\Gamma e} - V_{\Gamma e}^0$  and  $V_{\Gamma h} - V_{\Gamma h}^0$  for the electrons and holes in the  $\text{Al}_{0.34}\text{Ga}_{0.66}\text{As}$  layers and  $V_{Xe} - V_{Xe}^0$  for the electrons in the AlAs layers, respectively. The energy shift of the  $\Gamma$ - $\Gamma$  transition is determined by the sum of the second-order perturbed energy of the electrons and that of the holes, because the first-order perturbed energies cancel out each other. However, the  $X$ - $\Gamma$  transition energy shift is determined by the first-order perturbed energy between electrons and holes. From Fig. 3, we can intuitively understand the situation. As a result, the energy shifts of both the  $\Gamma$ - $\Gamma$  and  $X$ - $\Gamma$  energies are represented by

$$\begin{aligned} \Delta E_{\Gamma-\Gamma} &= -C(L_w^6/\hbar^2)[m_{\Gamma e}(4\pi e^2 n_h / \epsilon_{sw})^2 \\ &\quad + m_{\Gamma h}(4\pi e^2 n_h / \epsilon_{sw})^2], \end{aligned} \quad (3)$$

$$\Delta E_{X-\Gamma} = \frac{1}{12} [(4\pi e^2 n_h / \epsilon_{sw})L_w^2 + (4\pi e^2 n_e / \epsilon_{sb})L_b^2]. \quad (4)$$

Here,  $m_{\Gamma e}$  ( $m_{\Gamma h}$ ) and  $C$  denote the effective mass of an electron (a heavy hole) in the  $\Gamma$  point of the  $\text{Al}_{0.34}\text{Ga}_{0.66}\text{As}$  layers and a constant derived from the perturbation calculation, respectively. The result of the calculation for  $\Delta E_{\Gamma-\Gamma}$  is shown in Fig. 2 with a dashed line. Here, no adjustable parameters are used. If the density  $n_h$  increases slightly, the  $\Gamma$ - $\Gamma$  energy shift is well explained by our model, except for saturation of the redshift. Saturation of the redshift is simply explained by saturation of the  $X$  state. However, in this model the energy of the  $X$ - $\Gamma$  transition should shift toward high energy. The reason why the energy does not shift in the static luminescence measurement is considered as follows.

The duration of the transient band bending is determined by the decrease of the carrier's density and its spatial distributions. The lifetime of the  $\Gamma$ - $\Gamma$  luminescence is shorter than 10 ps,<sup>8</sup> so that its luminescence peak energy is considered to represent the energy of the band-bending

state. However, the  $X$ - $\Gamma$  luminescence has a long lifetime ( $\sim 10 \mu\text{s}$ ), so that the band bending is hardly observed in the static luminescence spectra. Actually, we observed a blueshift of the  $X$ - $\Gamma$  transition in the transient luminescence spectrum. In this experiment, we used the time-correlated single-photon counting method with a 0.9 ns time resolution. As a photoexcitation source, the cavity-dumped dye laser was used under 820 kHz operation. The excitation density was about  $10 \mu\text{J cm}^{-2}$ . Figure 4 shows the results of the stationary luminescence intensity (solid line) and the transient luminescence intensity at 0 ns (solid circles) around the  $X$ - $\Gamma$  transition energy. The  $\Gamma$ - $\Gamma$  luminescence peak energy under low-density limit excitation is indicated by an arrow in the inset. The result shows that the  $X$ - $\Gamma$  energy definitely shifts within the initial 0.9 ns. Calculation based on Eq. (4) shows that the blueshift of the  $X$ - $\Gamma$  energy is 6.5 meV under the excitation of  $10 \mu\text{J/cm}^2$ . The measured blueshift of the  $X$ - $\Gamma$  luminescence, 2 meV, is smaller than the expected value. In contrast to the blue-shifted spectrum with zero time delay, a spectrum with some time delay (1  $\mu\text{s}$ , for example) does not show a blueshift. These observations are probably explained by considering that the transient band bending ends faster than the present time resolution of 0.9 ns.

The saturation of the  $X$ - $\Gamma$  luminescence intensity and a limited redshift of the  $\Gamma$ - $\Gamma$  luminescence indicate that the upper limit of the  $X$ -point carrier density exists. The upper limit can be estimated from the saturation density of the  $X$ - $\Gamma$  luminescence intensity. We estimate it to be  $4 \times 10^{11} \text{ cm}^{-2}$  per layer (vertical arrow in Fig. 2). The reciprocal of this value is 16 nm, which corresponds closely to the exciton Bohr radius. This fact indicates that the excitons composed of  $X$  electrons in the AlAs layers and  $\Gamma$ -heavy holes in the  $\text{Al}_{0.34}\text{Ga}_{0.66}\text{As}$  layers are closely packed. As a result, the  $X$ - $\Gamma$  luminescence is saturated and the  $\Gamma$ - $\Gamma$  luminescence increases supralinearly. In this case, the  $\Gamma$ - $\Gamma$  recombination is the main relaxation process of the photoexcited carriers and the lifetime of the  $\Gamma$ - $\Gamma$  luminescence increases.<sup>11</sup>

The transient band bending is considered to be weakened for the following three reasons. One is the breakdown of the uniform distribution. In our calculation, we assumed that the electrons in the AlAs layers and holes in the  $\text{Al}_{0.34}\text{Ga}_{0.66}\text{As}$  layers are uniformly distributed. Initially, the assumption is probably correct, because the electrons and holes have enough kinetic energy. However, once the potential profile is bent as shown in Fig. 3, the electrons and holes are considered to localize near the interfaces. As a result, the band bending is weakened and the energy shift become small.

Another reason is the formation of interlayer excitons.<sup>9</sup> In our calculation of the energy shift, we assumed a homogeneous density distribution in the plane of the layers. However, the line of the Coulomb electric field between the electrons and holes can be short terminated if the  $X$  electrons are cooled and the  $X$ - $\Gamma$  indirect excitons are successively formed. In this case the effective electric field is reduced.

The third reason is the spatial diffusion of carriers.

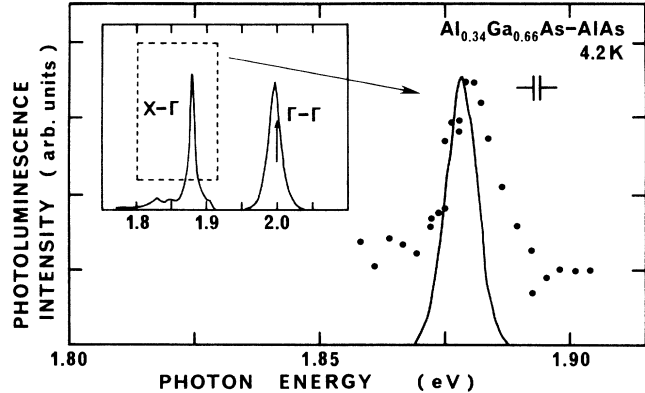


FIG. 4. Time-integrated and time-resolved spectra of the  $X$ - $\Gamma$  luminescence. The inset shows the entire time-integrated spectrum. The area surrounded by a dashed line in the inset is expanded. The time-integrated luminescence spectra are shown by solid lines and the  $X$ - $\Gamma$  transient luminescence spectrum is shown by solid circles. The transient luminescence corresponds to the time-resolved spectrum within the initial 0.9 ns obtained by using the time-correlated single-photon counting method. The data was obtained under  $10 \mu\text{J cm}^{-2}$  excitation. The vertical arrow in the inset represents the  $\Gamma$ - $\Gamma$  luminescence peak energy under low-density limit excitation.

Carrier diffusion is considered to reduce the carrier density. All of the above-mentioned reasons contribute to weaken the transient band bending, but it is difficult to determine the main contribution.

One considers that the redshift of the  $\Gamma$ - $\Gamma$  transition may come from the formation of the electron-hole plasma (EHP) or liquid (EHL). In type-I superlattices or MQW, the band-gap renormalization (BGR) reduces the band gap gradually. This reduction increases in proportion to  $n_{2D}^{1/3}$ ,<sup>12</sup> where  $n_{2D}$  represents the two-dimensional (2D) carrier density. The observed critical increase and saturation of the redshift are not explained by the formation of EHP or EHL. Although the  $X$ - $\Gamma$  energy of EHP or EHL in type-II MQW is considered to behave differently from the  $\Gamma$ - $\Gamma$  energy in type-I MQW,<sup>13</sup> the BGR of the  $\Gamma$ - $\Gamma$  transition in type-II MQW should be similar to that of type-I MQW. Therefore, the critical redshift and saturation of the redshift in the  $\Gamma$ - $\Gamma$  transition energy are not explained by the formation of EHP or EHL.

In short-period superlattices, such transient band bending cannot be observed.<sup>1</sup> One possible origin may be the narrow well width, where the energy shift cannot be resolved. Another reason may be miniband formation in short period superlattices.

In summary, we investigated the interlayer  $\Gamma$ - $X$  scattering process in staggered-alignment type-II  $\text{Al}_{0.34}\text{Ga}_{0.66}\text{As-AlAs}$  MQW. We observed a redshift for the  $\Gamma$ - $\Gamma$  luminescence and saturation for the  $X$ - $\Gamma$  luminescence under the same excitation density. Simultaneously, a blueshift of the  $X$ - $\Gamma$  luminescence was observed in the time-resolved luminescence spectra. These phenomena show the transient band bending caused by the interlayer  $\Gamma$ - $X$  transfer of electrons across the interfaces.

- <sup>1</sup>P. Saeta, J. F. Federici, R. J. Fischer, B. I. Greene, L. Pfeiffer, R. C. Spitzer, and B. A. Wilson, *Appl. Phys. Lett.* **54**, 1681 (1989).
- <sup>2</sup>J. Feldmann, R. Sattmann, E. O. Göbel, J. Kuhl, J. Hebling, K. Ploog, R. Muralidharan, P. Dawson, and C. T. Foxon, *Phys. Rev. Lett.* **62**, 1892 (1989).
- <sup>3</sup>Y. Masumoto, T. Mishina, F. Sasaki, and M. Adachi, *Phys. Rev. B* **40**, 8581 (1989).
- <sup>4</sup>M. V. Klein, M. D. Sturge, and E. Cohen, *Phys. Rev. B* **25**, 4331 (1982).
- <sup>5</sup>F. Minami, K. Hirata, K. Era, T. Yao, and Y. Masumoto, *Phys. Rev. B* **36**, 2875 (1987).
- <sup>6</sup>B. A. Wilson, C. E. Bonner, R. C. Spitzer, P. Dawson, K. J. Moore, and C. T. Foxon, *J. Vac. Sci. Technol. B* **6**, 1156 (1988).
- <sup>7</sup>B. A. Wilson, C. E. Bonner, R. C. Spitzer, R. Fischer, P. Dawson, K. J. Moore, C. T. Foxon, and G. W. 't Hooft, *Phys. Rev. B* **40**, 1825 (1989).
- <sup>8</sup>Y. Masumoto, T. Mishina, and F. Sasaki, *J. Lumin.* **45**, 189 (1990).
- <sup>9</sup>T. Mishina, F. Sasaki, and Y. Masumoto, *J. Phys. Soc. Jpn.* **59**, 2635 (1990).
- <sup>10</sup>Y. Masumoto and T. Tsuchiya, *J. Phys. Soc. Jpn.* **57**, 4403 (1988).
- <sup>11</sup>F. Sasaki, T. Mishina, and Y. Masumoto (unpublished).
- <sup>12</sup>G. Tränkle, H. Leier, A. Forchel, H. Haug, C. Ell, and G. Weimann, *Phys. Rev. Lett.* **58**, 419 (1987).
- <sup>13</sup>P. Hawrylak, *Phys. Rev. B* **39**, 6246 (1989).